Synthesis, Characterization, and Electrochemical Properties of Molecular Rectangles of Half-Sandwich Iridium Complexes Containing Bridging Chloranilate Ligands†

Ying-Feng Han, Yue-Jian Lin, Wei-Guo Jia, and Guo-Xin Jin*

Shanghai Key Laboratory of Molecular Catalysis and Innovative Material, Department of Chemistry, Fudan University, Shanghai, 200433, People's Republic of China

Received May 9, 2008

Binuclear complex $[Cp^*_2Ir_2(\mu\text{-CA})Cl_2]$ (**2**) (CA = chloranilate) was obtained by the reaction of $[Cp^*IrCl_2]_2$ (**1**) with H_2CA in the presence of base. Treatment of **2** with pyridine or 4-(4-bromophenyl)pyridine in the presence of AgOTf (OTf = CF_3SO_3) in CH_3OH gave the corresponding binuclear complexes $[Cp^*_2Ir_2(\mu\text{-CA})(\text{pyridine})_2](OTf)_2$ (**4a**) and $[Cp^*_2Ir_2(\mu\text{-CA})\{4\text{-(4-bromophenyl) pyridine}\}_2](OTf)_2$ (**4b**). Reactions of **2** with bidentate ligands gave tetranuclear complexes $[Cp^*_4Ir_4(\mu\text{-CA})_2(\mu\text{-L})_2](OTf)_4$ (L = pyrazine, **5a**; 4,4′-dipyridyl, **5b**; 2,5-bis(4-pyridyl)-1,3,5-oxadiazole, **5c**; 1,4-bis(4-pyridyl)benzene, **5d**; (*E*)-1,2-bis(4-pyridyl)ethene, **5e**). X-ray analyses of **5a**, **5b**, and **5e** revealed that each of four Cp*Ir moieties was connected by pyridyl ligands and a bis-bidentate chloranilate (CA) ligand to construct a rectangular cavity with the dimensions 8.03 × 6.92 Å for **5a**, 8.03 × 11.24 Å for **5b**, and 8.01 × 13.55 Å for **5e**. Toluene molecules are contained as solvent molecules in the crystals of **5a** and **5b**. For **5a**, the toluene molecules appeared between the independent rectangles, but the toluene molecules appeared in the rectangle cavity for **5b**. The electrochemical properties of **5b** and **5e** were investigated preliminarily, using cyclic voltammetry.

Introduction

Metal complexes with 1,4-dihydroxybenzoquinonediide and its homologues have been widely studied because they can provide a variety of binding sites for metal cations and charged states. The dianionic form has five coordination modes, which afford intriguing crystal structures and physicochemical properties.[1] It is well-known that the dianion of 2,5-dichloro-3,6-dihydroxy-1,4-benzoquinone (chloranilic acid, H_2CA) can coordinate with metal ions in both the bidentate and the bis-bidentate fashions, and the coordination compounds containing chloranilate (CA) as bis-bidentate ligands have been prepared and studied extensively.[1−15] The bis form essentially provides a one-dimensional framework, but when another linking ligand is used, a two-dimensional one can be obtained. However, metal compounds with the chloranilate ligand to build two-dimensional organometallic rectangles have not been reported, although these supramolecular structures may display interesting functional properties and applications in various fields, including host−guest chemistry, redox activity, magnetic behavior, photo- and electrochemical sensing, and catalysis.

† Dedicated to Professor Xi-Yan Lu on the occasion of his 80th birthday.

* Corresponding author. Tel: +86-21-65643776. Fax: + 86-21-65641740. E-mail: gxjin@fudan.edu.cn.

(1) Kitagawa, S.; Kawata, S. *Coord. Chem. Rev.* **2002**, *224*, 11.
(2) Kabir, M. K.; Miyazaki; Kawata, N.; S.; Adachi, K.; Kumagai, H.; Inoue, K.; Kitagawa, S.; Iijima, K. *Coord. Chem. Rev.* **2000**, *198*, 157.
(3) Yoshino, A.; Matsudaira, H.; Asato, E.; Koikawa, M.; Shiga, T.; Ohba, M.; Okawa, H. *Chem. Commun.* **2002**, 1258.
(4) Gregorio, S.; Jorge, V.; Gregorio, L.; Luis, S. J.; Luis, G.; Jose, P. *Eur. J. Inorg. Chem.* **2005**, *12*, 2360.
(5) Prithwiraj, B. *Trans. Metal Chem.* **2005**, *30*, 738.
(6) Luo, T.-T.; Liu, Y.-H.; Tsai, H.-L.; Su, C.-C.; Ueng, C.-H.; Lu, K.-L. *Eur. J. Inorg. Chem.* **2004**, *21*, 4253.
(7) (a) Heinze, K.; Huttner, G.; Zsolnai, L.; Jacobi, A.; Schober, P. *Chem.−Eur.J.* **1997**, *3*, 32. (b) Heinze, K.; Huttner, G.; Walter, O. *Eur. J. Inorg. Chem.* **1999**, 593.
(8) Carbonera, C.; Dei, A.; Lëtard, J.-F.; Sangregorio, C.; Sorace, L. *Angew. Chem., Int. Ed.* **2004**, *43*, 3136.
(9) Tao, J.; Maruyama, H.; Sato, O. *J. Am. Chem. Soc.* **2006**, *128*, 1790.
(10) Gupta, P.; Das, A.; Basuli, F.; Castineiras, A.; Sheldrick, W. S.; Mayer-Figge, H.; Bhattacharya, S. *Inorg. Chem.* **2005**, *44*, 2081.
(11) Jasimuddin, S.; Byabartta, P.; Sinha, C.; Mostafa, G.; Lu, T. H. *Inorg. Chim. Acta* **2004**, *357*, 2015.
(12) Kawahara, M.; Kabir, M. K.; Yamada, K.; Adachi, K.; Kumagai, H.; Narumi, Y.; Kindo, K.; Kitagawa, S.; Kawata, S. *Inorg. Chem.* **2004**, *43*, 92.
(13) Nagayoshi, K.; Kabir, M. K.; Tobita, H.; Honda, K.; Kawahara, M.; Katada, M.; Adachi, K.; Nishikawa, H.; Ikemoto, I.; Kumagai, H.; Hosokoshi, Y.; Inoue, K.; Kitagawa, S.; Kawata, S. *J. Am. Chem. Soc.* **2003**, *125*, 221.
(14) Min, K. S.; Rheingold, A. L.; DiPasdquale, A.; Miller, J. S. *Inorg. Chem.* **2006**, *45*, 6135.
(15) Min, K. S.; DiPasdquale, A.; Goled, J. A.; Rheingold, A. L.; Miller, J. S. *J. Am. Chem. Soc.* **2007**, *129*, 2360.
(16) (a) Fish, R. H.; Jaouen, G. *Organometallics* **2003**, *22*, 2166. (b) Fish, R. H *Coord. Chem. Rev.* **1999**, *185−186*, 569. (c) Korn, S.; Sheldrick, W. S. *Dalton Trans.* **1997**, 2191. (d) Yamanari, K.; Ito, R.; Yamamoto, S.; Konno, T.; Fuyuhiro, A.; Kobayashi, M.; Arakawa, R. *Dalton Trans.* **2003**, 380. (e) Yamanari, K.; Ito, R.; Yamamoto, S.; Fuyuhiro, A. *Chem. Comm.* **2001**, 1414.
(17) Boyer, J. L.; Kuhlman, M. L.; Rauchfuss, T. B. *Acc. Chem. Res.* **2007**, *40*, 233.
(18) Severin, K. *Chem. Commun.* **2006**, 3859.
(19) (a) Han, Y.-F.; Lin, Y.-J.; Jia, W.-G.; Weng, L.-H.; Jin, G.-X *Organometallics* **2007**, *26*, 5848. (b) Han, Y.-F.; Jia, W.-G.; Lin, Y.-J.; Jin, G.-X. *J. Organomet. Chem.* **2008**, *693*, 546. (c) Wang, J.-Q.; Ren, C.-X.; Jin, G.-X. *Organometallics* **2006**, *25*, 74. (d) Wang, J.-Q.; Zhang, Z.; Weng, L.-H.; Jin, G.-X. *Chin. Sci. Bull.* **2004**, *49*, 1122.
(20) (a) Yan, H.; Süss-Fink, G.; Neels, A.; Stoeckli-Evans, H. *Dalton Trans.* **1997**, 4345. (b) Govindaswamy, P.; Linder, D.; Lacour, J.; Süss-Fink, G.; Therrien, B *Chem. Commun.* **2006**, 4691. (c) Suzuki, H.; Tajima, N.; Tatsumi, K.; Yamamoto, Y. *Chem. Commun.* **2000**, 1801. (d) Yamamotoa, Y.; Suzuki, H.; Tajima, N.; Tatsumi, K. *Chem.−Eur. J.* **2002**, *8*, 372.
(21) Han, Y.-F.; Lin, Y.-J.; Weng, L.-H.; Berke, H.; Jin, G.-X. *Chem. Commun.* **2008**, 350.

10.1021/om800426e CCC: $40.75
Publication on Web 07/31/2008

Scheme 1. Synthesis of Binuclear Complexes 2, 3, 4a, and 4b

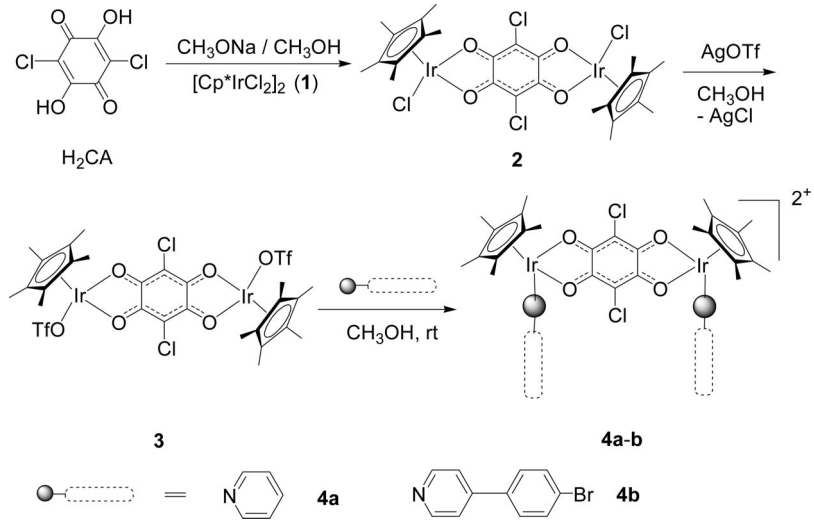

In previous work, the design and synthesis of metal-containing supramolecules with organometallic half-sandwich complexes based on Ir, Rh, and Ru fragments have been developed by many groups.[16−18] We[19] and others[20] have reported the stepwise formation of tetra- and hexanuclear iridium and rhodium complexes bearing organic π-ligands and oxalato bridges, connected by two and three pyridyl-based subunits. The stepwise formation of "organometallic boxes" with half-sandwich Ir, Rh, and Ru fragments also has been realized in our group recently.[21] The general design strategy for the formation of molecular architectures involves the design of a binuclear complex with two parallel coordination sites, and the complexes contain two-dimensional architectures with two different ligand "edges".

Herein we report the stepwise formation of bi- and tetranuclear iridium complexes bearing pentamethylcyclopentadienyl and chloranilate bridges, based on pyridyl-based subunits. A new series of bi- and tetranuclear iridium complexes were synthesized and characterized. Binuclear complexes $[Cp^*_2Ir_2(\mu\text{-}CA)Cl_2]$ (**2**) and $[Cp^*_2Ir_2(\mu\text{-}CA)\{4\text{-}(4\text{-bromophenyl})\text{pyridine}\}_2](OTf)_2$ (**4b**) and tetranuclear complexes $[Cp^*_4Ir_4(\mu\text{-}CA)_2(\mu\text{-pyrazine})_2](OTf)_4$ (**5a**), $[Cp^*_4Ir_4(\mu\text{-}CA)_2(\mu\text{-}4,4'\text{-dipyridyl})_2](OTf)_4$ (**5b**), and $[Cp^*_4Ir_4(\mu\text{-}CA)_2\{\mu\text{-}(E)\text{-}1,2\text{-bis}(4\text{-pyridyl})\text{ethene}\}_2(OTf)_4$ (**5e**) ($Cp^* = \eta^5\text{-}C_5Me_5$) were confirmed by X-ray analyses. The cyclic voltammograms of **5b** and **5e** exhibit good electrochemical responses, two obvious cathodic peaks and two anodic peaks can be observed in **5b**, and the CV of **5e** shows three well-separated quasi-reversible one-electron transfer waves.

Results and Discussion

Synthesis and Characterization. The ligands 4-(4-bromophenyl)pyridine and 1,4-bis(4-pyridyl)benzene were prepared via Suzuki coupling reactions between 1,4-dibromobenzene and pyridine 4-boronic acid in 1:1 or 1:3 molar ratios in the presence of base, respectively.

Table 1. Selected Bond Distances and Angles for 2

Bond Distances (Å)			
Ir(1)−O(1)	2.116(3)	Ir(1)−O(2)	2.140(3)
Ir(1)−Cl(2)	2.3845(14)	O(1)−C(2)	1.276(5)
O(2)−C(1)	1.265(5)	C(1)−C(2)	1.516(6)
C(2)−C(3)	1.381(6)	Cl(1)−C(3)	1.729(4)
Ir(1)−C(4)	2.147(5)	Ir(1)−C(5)	2.140(4)
Ir(1)−C(6)	2.136(5)	Ir(1)−C(7)	2.136(5)
Bond Angles (deg)			
O(1)−Ir(1)−C(8)	119.87(15)	O(1)−Ir(1)−C(7)	96.88(15)
C(8)−Ir(1)−C(7)	39.24(18)	O(1)−Ir(1)−C(6)	108.40(15)
C(8)−Ir(1)−C(6)	66.41(18)	C(7)−Ir(1)−C(6)	39.61(18)
O(1)−Ir(1)−C(5)	145.72(16)	C(8)−Ir(1)−C(5)	65.82(17)
C(7)−Ir(1)−C(5)	65.87(17)	C(6)−Ir(1)−C(5)	39.57(18)
O(1)−Ir(1)−O(2)	75.67(11)	C(8)−Ir(1)−O(2)	163.69(15)
C(7)−Ir(1)−O(2)	140.75(16)	C(6)−Ir(1)−O(2)	105.42(15)
C(5)−Ir(1)−O(2)	98.70(14)	O(1)−Ir(1)−C(4)	159.59(16)
C(8)−Ir(1)−C(4)	39.73(18)	C(7)−Ir(1)−C(4)	66.06(18)
C(6)−Ir(1)−C(4)	66.19(18)	C(5)−Ir(1)−C(4)	38.74(18)
O(2)−Ir(1)−C(4)	124.56(15)	O(1)−Ir(1)−Cl(2)	84.77(10)
O(2)−Ir(1)−Cl(2)	85.46(9)	C(2)−O(1)−Ir(1)	116.6(3)
C(1)−O(2)−Ir(1)	115.6(3)	O(2)−C(1)−C(2)	116.0(4)
O(1)−C(2)−C(1)	115.0(4)	C(3)−C(2)−C(1)	120.8(4)

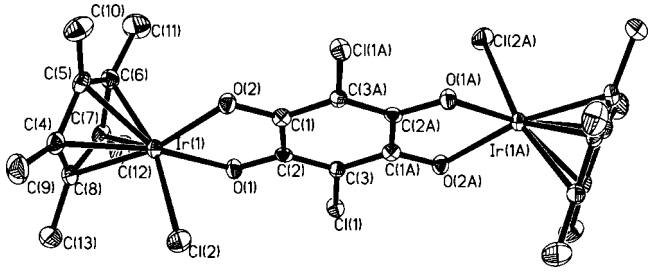

Figure 1. Molecular structure of complex **2** with thermal ellipsoids drawn at the 50% level. All hydrogen atoms are omitted for clarity.

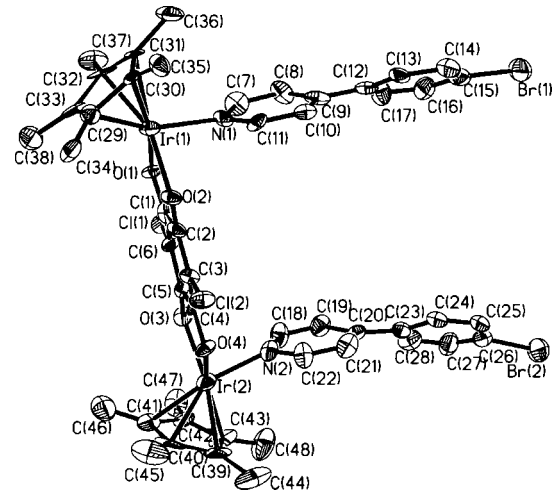

Figure 2. Complex cation of **4b** with thermal ellipsoids drawn at the 50% level. All hydrogen atoms, anions, and solvent molecules are omitted for clarity.

Table 2. Selected Bond Distances and Angles for 4b

Bond Distances (Å)			
Ir(1)−O(1)	2.112(10)	Ir(1)−O(2)	2.124(10)
Ir(2)−O(3)	2.136(11)	Ir(2)−O(4)	2.101(10)
Ir(1)−N(1)	2.116(13)	Ir(2)−N(2)	2.106(14)
O(1)−C(1)	1.256(17)	O(2)−C(2)	1.280(17)
O(3)−C(5)	1.238(18)	O(4)−C(4)	1.264(17)
C(1)−C(2)	1.52(2)	C(1)−C(6)	1.39(2)
C(2)−C(3)	1.38(2)	C(3)−C(4)	1.40(2)
C(4)−C(5)	1.50(2)	C(5)−C(6)	1.40(2)
Cl(1)−C(6)	1.746(16)	Cl(2)−C(3)	1.715(14)
Br(1)−C(15)	1.881(18)	Br(2)−C(26)	1.925(18)
Bond Angles (deg)			
O(1)−Ir(1)−N(1)	84.5(4)	N(1)−Ir(1)−O(2)	85.4(4)
O(4)−Ir(2)−N(2)	85.5(5)	N(2)−Ir(2)−O(3)	82.4(5)
O(1)−Ir(1)−O(2)	75.8(4)	O(4)−Ir(2)−O(3)	76.1(4)
C(1)−O(1)−Ir(1)	116.9(9)	C(2)−O(2)−Ir(1)	116.8(9)
C(5)−O(3)−Ir(2)	114.3(10)	C(4)−O(4)−Ir(2)	116.5(10)
C(7)−N(1)−Ir(1)	121.7(11)	C(11)−N(1)−Ir(1)	120.0(10)
C(18)−N(2)−Ir(2)	121.4(12)	C(22)−N(2)−Ir(2)	119.7(12)
O(1)−C(1)−C(2)	116.3(13)	O(1)−C(1)−C(6)	126.5(13)
C(6)−C(1)−C(2)	117.2(13)	O(2)−C(2)−C(3)	124.0(14)
O(2)−C(2)−C(1)	114.1(13)	C(3)−C(2)−C(1)	121.8(13)
C(2)−C(3)−C(4)	118.9(13)	C(2)−C(3)−Cl(2)	122.3(11)
C(4)−C(3)−Cl(2)	118.8(11)	O(4)−C(4)−C(3)	123.9(14)
O(4)−C(4)−C(5)	114.7(13)	C(3)−C(4)−C(5)	121.4(13)
O(3)−C(5)−C(6)	123.8(15)	O(3)−C(5)−C(4)	118.2(13)
C(6)−C(5)−C(4)	118.0(14)	C(1)−C(6)−C(5)	122.5(14)
C(1)−C(6)−Cl(1)	117.3(11)	C(5)−C(6)−Cl(1)	120.2(12)

Binuclear Complexes. As shown in Scheme 1, when bis[dichloro(pentamethylcyclopentadienyl)iridium(III)] (**1**) was treated with H_2CA in the presence of CH_3ONa in a 1:1:2 molar ratio in CH_3OH at room temperature, red crystals of the binuclear complex (**2**) were formed in high yield, and the complex is soluble in CH_2Cl_2. The IR spectra showed a strong band at approximately 1496 cm^{-1}, owing to the C═O stretching of the bridging chloranilate ligands. The ^1H NMR spectra showed a sharp singlet at about $\delta = 1.67$ ppm due to the Cp* protons. These spectroscopic data and the combustion analyses for C and H indicate a dimeric structure in which the Ir centers are connected by a chloranilate as bis-bidentate ligands. The coordinative unsaturated intermediate **3** can be obtained by the reaction of **2** with 2 equiv of AgOTf in CH_3OH at room temperature after separation from AgCl. The synthesis route is similar to our previous report for synthesis of the binuclear oxalate complex $[Cp^*_2Ir_2(\mu\text{-}\eta^4\text{-}C_2O_4)](OTf)_2$.[19a,21]

The molecular structure of **2** has been determined by X-ray diffraction methods using a single crystal obtained by slow diffusion of hexane into a concentrated solution of the complex in CH_2Cl_2 at low temperature. A perspective drawing of **2** with the atomic numbering scheme is given in Figure 1, and selected bond lengths and angles are listed in Table 1. The crystal structure of **2** consists of binuclear units, connected by a chloranilate ligand, and each iridium atom is surrounded by two O atoms of CA and one Cl atom. All of the iridium centers have six-coordinate geometry, assuming that the Cp* ligand functions as a three-coordinate ligand. The average $Ir-C_{Cp^*}$ bond distance is 2.136 Å, which compares well with that for other iridium complexes containing Cp* rings. The average Ir−O bond distance is 2.128 Å, which falls well within the range of that observed for typical M−O coordination compounds containing chloranilate as bis-bidentate ligands.[1]

The chloranilate C1−C2 and average C−O bond distances are 1.516(6) and 1.271 Å, respectively, and are characteristic of CA (vide infra).[22] The average bite distance of the chloranilate five-membered chelate ring is 2.611 Å. The shortest intradimer Ir···Ir separation is 8.045 Å, and it is 18% longer than the shortest interdimer Ir···Ir separation of 6.594 Å. In addition, the iridium atom is 0.2614 Å out of the chloranilate coordination plane, and the two Cl atoms are oriented in a *trans* manner.

Treatment of **2** with pyridine or 4-(4-bromophenyl)pyridine in the presence of AgOTf in CH_3OH at room temperature gave binuclear complexes, formulated as $[Cp^*_2Ir_2(\mu\text{-CA})(\text{pyridine})_2](OTf)_2$ (**4a**) and $[Cp^*_2Ir_2(\mu\text{-CA})\{4\text{-(4-bromophenyl)pyridine}\}_2](OTf)_2$ (**4b**), respectively, in high yields. The IR spectra showed a bridging chloranilate band at approximately 1509 for **4a** and 1506 cm^{-1} for **4b**. The ^1H NMR spectra for **4a** showed a singlet at about $\delta = 1.68$ ppm due to the Cp* protons and multiple resonances in the range $\delta = 7.64-8.65$ ppm due to pyridine protons, indicating the presence of a configurational isomer; that for **4b** exhibited a singlet at about $\delta = 1.67$ ppm due to the Cp* protons and four complex resonances of pyridyl protons, indicating the presence of a configurational isomer, as did that in the case of **4a**. The detailed structure was confirmed by X-ray analysis of **4b** (Figure 2), and selected bond lengths and angles are listed in Table 2. The asymmetric unit of **4b** contains one $[Cp^*_2Ir_2(\mu\text{-CA})\{4\text{-(4-bromophenyl)pyridine}\}_2]^{2+}$ cation as well as two triflate coun-

Scheme 2. Synthesis of Tetranuclear Complexes 5a−5e

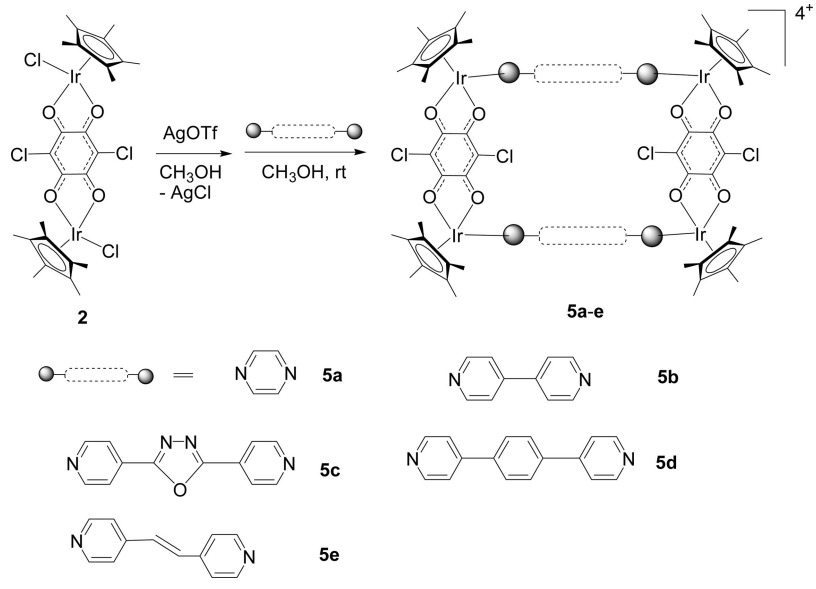

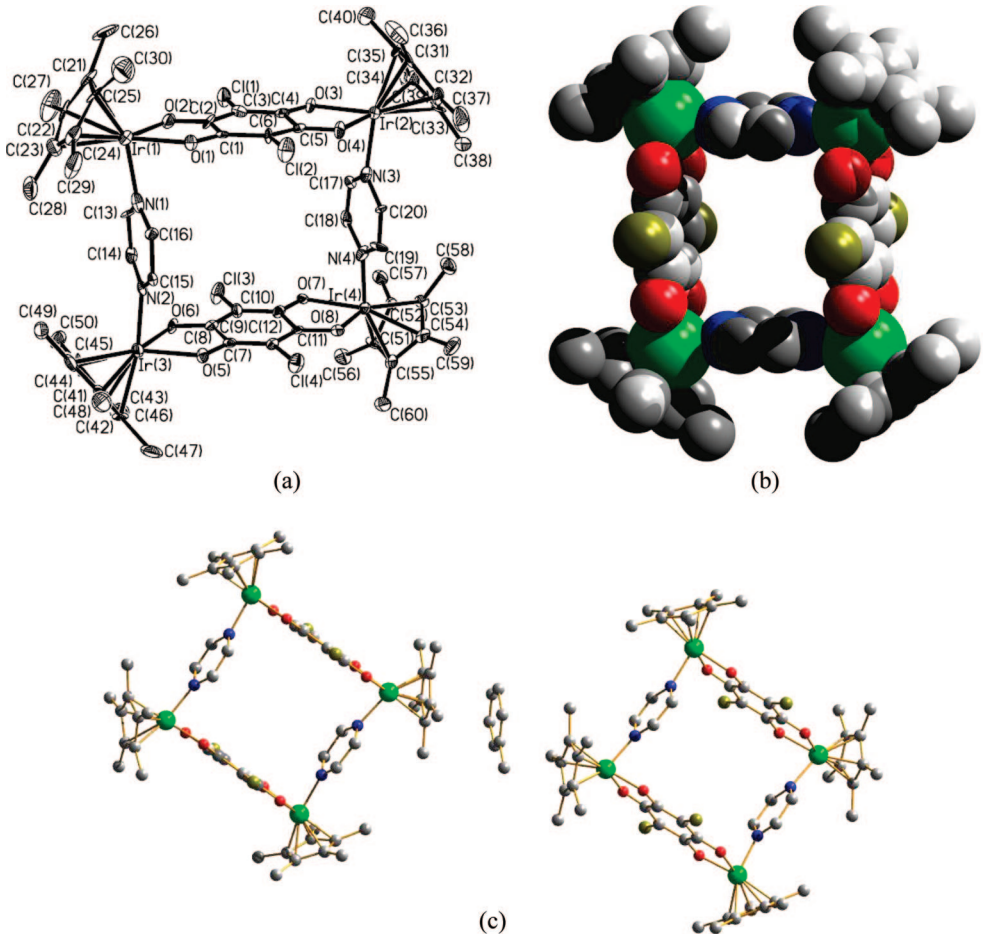

Figure 3. (a) Complex cation of **5a** with thermal ellipsoids drawn at the 30% level. (b) Space-filling model of cationic molecular rectangle **5a** based on its X-ray coordinates. All hydrogen atoms, anions, and solvent molecules are omitted for clarity. (c) Stacking of the molecules in crystals of **5a** showing $\pi-\pi$ interactions between Cp* rings and toluene molecules (Ir green; O red; N blue; C gray; Cl dark yellow). All hydrogen atoms, anions, and other solvent molecules are omitted for clarity.

teranions in the solid state. As illustrated in Figure 2, two Cp* rings are *syn* to each other and the two 4-(4-bromophenyl) pyridine ligands are parallel to each other in a *syn* manner. A similar conformation also can be found in other binuclear complexes, such as the Ir(III) complex $[(Cp^*IrCl_2)_2(\mu\text{-pyrazine})]$ and the Rh(III) complex $[Cp^*Rh(\eta^1\text{-}NO_3)_2(\mu\text{-pyrazine})_{0.5}]_2$.[19c,23]

The average Ir−N and Ir−O bond distances are 2.111 and 2.118 Å, respectively. The chloranilate C1−C2 and average C−O bond distances are 1.52(2) and 1.259 Å, respectively. These bond distances are similar to those for **2**. The average bite distance of the chloranilate five-membered chelate ring is 2.61 Å. The two Ir atoms are separated by 8.026 Å.

Tetranuclear Complexes. As shown in Scheme 2, tetranuclear complex **5a**, which bears the pyrazine ligand and is formulated as $[Cp^*_4Ir_4(\mu\text{-pyrazine})_2(CA)_2](OTf)_4$, was prepared by direct reactions of **2** with pyrazine in the presence of AgOTf. Complex **5a** is soluble in CH_3OH but almost insoluble in CH_2Cl_2. The IR showing a strong band at 1508 cm^{-1} indicates the presence of the coordinated chloranilate ligands. The ^1H NMR spectrum for **5a** in CD_3OD showed two singlets at $\delta =$ 1.67 ppm due to Cp* protons and $\delta = 8.7$ ppm due to pyrazine protons. The detailed structure was confirmed by X-ray analyses of **5a** (Figure 3), and selected bond lengths and angles are listed in Table 3. The complex cation has a rectangular structure bridged by two chloranilate ligands and two pyrazine molecules. The crystal structure of **5a** is composed of one $[Cp^*_4Ir_4(\mu\text{-pyrazine})_2(CA)_2]^{4+}$ cation, four triflate counteranions, and CH_3OH, CH_2Cl_2, H_2O, and toluene solvent molecules in the solid. Each Ir atom is coordinated by one nitrogen atom from pyrazine and two oxygen atoms of chloranilate ligands, resulting in a tetranuclear rectangle structure, with the dimensions 8.03 × 6.92 Å, as defined by the iridium centers, and the Ir(1)···Ir(4) and Ir(2)···Ir(3) diagonal lengths in the rectangular structure are 10.61 and 10.58 Å, respectively. The average Ir−N and Ir−O bond distances are 2.076 and 2.124 Å, respectively. The chloranilate C1−C2 and average C−O bond distances are 1.523(19) and 1.272 Å, respectively.[15] The average bite distance of the chloranilate five-membered chelate ring is 2.645 Å. The shortest intradimer Ir···Ir separation is 8.031 Å, and it is 9% less than the shortest interdimer Ir···Ir separation of 8.991 Å. In addition, the iridium atoms are 0.0371, 0.0208, 0.0231, and 0.0988 Å out of the corresponding chloranilate coordination plane.

As shown in Figure 3c, the molecular rectangles can stabilize via the $\pi-\pi$ interactions between Cp* rings and toluene molecules with a distance of 3.6 Å. On the other hand, the molecular rectangles stack to form rectangle channels due to the $\pi-\pi$ interactions between the independent molecules.[19a] The overall free voids are 17.8% of the cell volume, which is calculated on the condition that counteranions, solvent molecules, and hydrogen atoms are omitted. In addition, the CH_2Cl_2

(22) (a) Kennedy, A. R.; Waterson, F. R. N. *Acta Crystallogr.* **2003**, *C59*, o613. (b) Ishida, H.; Kashino, S. *Acta Crystallogr.* **2001**, *C57*, 476.
(23) Han, W. S.; Lee, S. W. *Dalton Trans.* **2004**, 1656.

Table 3. Selected Bond Distances and Angles for 5a

Bond Distances (Å)			
Ir(1)−O(1)	2.124(9)	Ir(1)−O(2)	2.117(10)
Ir(2)−O(3)	2.139(8)	Ir(2)−O(4)	2.101(10)
Ir(3)−O(5)	2.140(8)	Ir(3)−O(6)	2.115(10)
Ir(4)−O(7)	2.139(8)	Ir(4)−O(8)	2.116(9)
Ir(1)−N(1)	2.090(14)	Ir(2)−N(3)	2.073(13)
Ir(3)−N(2)	2.063(11)	Ir(4)−N(4)	2.079(12)
O(1)−C(1)	1.278(15)	O(2)−C(2)	1.277(15)
O(3)−C(4)	1.258(16)	O(4)−C(5)	1.246(14)
O(5)−C(7)	1.284(14)	O(6)−C(8)	1.269(14)
O(7)−C(10)	1.273(15)	O(8)−C(11)	1.294(14)
C(1)−C(2)	1.523(19)	C(2)−C(3)	1.400(19)
C(3)−C(4)	1.390(19)	C(4)−C(5)	1.563(19)
C(5)−C(6)	1.375(18)	C(1)−C(6)	1.409(16)
C(7)−C(8)	1.521(17)	C(8)−C(9)	1.406(18)
C(9)−C(10)	1.407(17)	C(10)−C(11)	1.530(17)
C(11)−C(12)	1.400(16)	C(7)−C(12)	1.369(16)
Bond Angles (deg)			
N(1)−Ir(1)−O(1)	84.4(4)	N(1)−Ir(1)−O(2)	86.2(4)
O(2)−Ir(1)−O(1)	77.0(3)	N(3)−Ir(2)−O(4)	86.5(4)
N(3)−Ir(2)−O(3)	84.9(4)	O(4)−Ir(2)−O(3)	77.2(3)
N(2)−Ir(3)−O(6)	83.0(4)	N(2)−Ir(3)−O(5)	84.4(4)
O(6)−Ir(3)−O(5)	76.6(3)	N(4)−Ir(4)−O(8)	82.2(4)
N(4)−Ir(4)−O(7)	85.3(4)	O(8)−Ir(4)−O(7)	77.2(3)
C(1)−O(1)−Ir(1)	115.0(8)	C(2)−O(2)−Ir(1)	116.2(9)
C(4)−O(3)−Ir(2)	115.0(8)	C(5)−O(4)−Ir(2)	116.4(9)
C(7)−O(5)−Ir(3)	115.0(7)	C(8)−O(6)−Ir(3)	116.5(8)
C(10)−O(7)−Ir(4)	114.5(8)	C(11)−O(8)−Ir(4)	116.2(8)
O(1)−C(1)−C(6)	124.9(13)	O(1)−C(1)−C(2)	116.7(11)
C(6)−C(1)−C(2)	118.3(13)	O(2)−C(2)−C(3)	123.8(14)
O(2)−C(2)−C(1)	115.1(12)	C(3)−C(2)−C(1)	121.1(12)
C(4)−C(3)−C(2)	119.7(14)	C(4)−C(3)−Cl(1)	119.4(12)

Table 4. Selected Bond Distances and Angles for 5b

Bond Distances (Å)			
Ir(1)−N(1)	2.128(8)	Ir(2)−N(2)	2.123(9)
Ir(3)−N(3)	2.102(8)	Ir(4)−N(4)	2.134(8)
Ir(1)−O(1)	2.104(7)	Ir(1)−O(2)	2.134(7)
Ir(2)−O(6)	2.133(7)	Ir(2)−O(5)	2.122(7)
Ir(3)−O(3)	2.120(7)	Ir(3)−O(4)	2.131(7)
Ir(4)−O(8)	2.134(6)	Ir(4)−O(7)	2.125(7)
O(1)−C(1)	1.257(11)	O(2)−C(2)	1.269(10)
O(3)−C(5)	1.277(11)	O(4)−C(4)	1.255(11)
O(5)−C(7)	1.294(11)	O(6)−C(8)	1.252(10)
O(7)−C(11)	1.267(11)	O(8)−C(10)	1.261(10)
C(1)−C(2)	1.501(13)	C(2)−C(3)	1.388(13)
C(3)−C(4)	1.351(12)	C(4)−C(5)	1.541(13)
C(5)−C(6)	1.423(14)	C(1)−C(6)	1.386(12)
C(7)−C(8)	1.553(13)	C(8)−C(9)	1.354(12)
C(9)−C(10)	1.411(12)	C(10)−C(11)	1.509(13)
C(11)−C(12)	1.370(13)	C(7)−C(12)	1.377(13)
Bond Angles (deg)			
O(1)−Ir(1)−N(1)	85.1(3)	O(1)−Ir(1)−O(2)	75.9(3)
N(1)−Ir(1)−O(2)	85.2(3)	O(5)−Ir(2)−N(2)	83.2(3)
O(5)−Ir(2)−O(6)	76.3(2)	N(2)−Ir(2)−O(6)	83.8(3)
N(3)−Ir(3)−O(3)	82.6(3)	N(3)−Ir(3)−O(4)	84.0(3)
O(3)−Ir(3)−O(4)	75.7(2)	O(7)−Ir(4)−O(8)	75.2(3)
O(7)−Ir(4)−N(4)	83.6(3)	O(8)−Ir(4)−N(4)	85.8(3)
C(1)−O(1)−Ir(1)	115.5(6)	C(2)−O(2)−Ir(1)	116.6(6)
C(5)−O(3)−Ir(3)	117.2(6)	C(4)−O(4)−Ir(3)	117.3(7)
C(7)−O(5)−Ir(2)	116.6(7)	C(8)−O(6)−Ir(2)	117.2(6)
C(11)−O(7)−Ir(4)	115.6(6)	C(10)−O(8)−Ir(4)	118.1(6)
O(1)−C(1)−C(6)	122.7(9)	O(1)−C(1)−C(2)	118.2(9)
C(6)−C(1)−C(2)	119.1(9)	O(2)−C(2)−C(3)	123.9(9)
O(2)−C(2)−C(1)	113.7(9)	C(3)−C(2)−C(1)	122.4(8)
O(4)−C(4)−C(3)	125.9(10)	O(4)−C(4)−C(5)	115.3(9)

molecules are seen in the molecular rectangles and H_2O and CH_3OH molecules also can be found in the rectangle channels, but the counteranions are located outside of the channels.

Analogously, the reactions of **2** with 4,4′-dipyridyl or 2,5-bis(4-pyridyl)-1,3,5-oxadiazole in the presence of AgOTf gave the corresponding tetranuclear complexes $[Cp^*_4Ir_4(\mu\text{-}4,4'\text{-dipyridyl})_2(CA)_2](OTf)_4$ (**5b**) and $[Cp^*_4Ir_4(\mu\text{-}2,5\text{-bis(4-pyridyl)-1,3,5-oxadiazole})_2(CA)_2](OTf)_4$ (**5c**). The IR, showing a strong band at 1511 cm^{-1} for **5b** and 1512 cm^{-1} for **5c**, also indicates the presence of the chloranilate ligands. The ^1H NMR spectra for **5b** showed a singlet at $\delta = 1.63$ ppm due to Cp* protons and two double resonances at ca. $\delta = 8.04$ and 8.53 ppm due to dipyridyl protons; that for **5c** had an analogous singlet at $\delta = 1.68$ ppm due to Cp* protons and two double resonances at ca. $\delta = 8.23$ and 8.65 ppm due to pyridyl protons. A perspective drawing of **5b** with the atomic numbering scheme is given in Figure 4, and selected bond lengths and angles are listed in Table 4. The complex has a rectangular structure with Ir···Ir lengths of 8.03 and 11.24 Å.

The average Ir−N and Ir−O bond distances are 2.122 and 2.125 Å, respectively. The chloranilate C1−C2 and average C−O bond distances are 1.501(13) and 1.266 Å, respectively. The average bite distance of the chloranilate five-membered chelate ring is 2.610 Å.[15] The shortest intradimer Ir···Ir separation is 8.026 Å, and it is 5.5% less than the shortest interdimer Ir···Ir separation of 8.493 Å. In addition, the iridium atoms are 0.0296, 0.0020, 0.0475, and 0.0150 Å out of the corresponding chloranilate coordination plane, as in the case of **5a**.

As shown in Figure 4c, unlike the molecular rectangles, which were stabilized via the $\pi-\pi$ interactions between Cp* rings and toluene molecules in complex **5a**, toluene molecule are stabilized in the cavity of the molecular rectangle complex **5b** due to $\pi-\pi$ interactions. To our surprise, the pyridyl rings of 4,4′-dipyridyl are tilted toward each other in complex **5b**; however, the two bpy ligands of $[Cp^*_4Ir_4(\mu\text{-bpy})_2(\mu\text{-}\eta^4\text{-}C_2O_4)_2](OTf)_4$ are parallel and close to each other.[19a] The overall free voids are 23.8% of the cell volume, which is calculated on the condition that counteranions, solvent molecules, and hydrogen atoms are omitted. In addition, the toluene molecules are seen in the rectangle channels, but the counteranions are located outside of the channels.

Similarly, tetranuclear complexes $[Cp^*_4Ir_4(\mu\text{-}1,4\text{-bis(4-pyridyl)benzene})_2(CA)_2](OTf)_4$ (**5d**) and $[Cp^*_4Ir_4(\mu\text{-(E)-1,2-bis(4-pyridyl)ethylene})_2(CA)_2](OTf)_4$ (**5e**) can be prepared readily from binuclear complex **2** and 1,4-bis(4-pyridyl)benzene or 1,2-bis(4-pyridyl)ethylene under similar experimental conditions in 56% and 67% yield, respectively. In the ^1H NMR spectra, the Cp* methyl protons appear at 1.69 ppm for **5d** and 1.66 ppm for **5e** as a singlet, while the resonances for the pyridyl are around $\delta = 7.73$, 7.96, 8.37, and 8.46 for the former and 7.52, 7.78, and 8.35 ppm for the latter. Both of them indicate high molecular symmetry in these complexes. The bands at around 1508 cm^{-1} for **5d** and 1504 cm^{-1} for **5e**, in the IR spectra, can be assigned to C═O stretching.

The structure of **5e** also has been determined by X-ray analyses. A perspective drawing of **5e** with the atomic numbering scheme is given in Figure 5, and selected bond lengths and angles are listed in Table 5. The complex has a rectangular structure with Ir···Ir lengths of 8.01 and 13.55 Å.

The average Ir−N and Ir−O bond distances are 2.072 and 2.129 Å, respectively. The chloranilate C1−C2 and average C−O bond distances are 1.508(15) and 1.257 Å, respectively. The average bite distance of the chloranilate five-membered chelate ring is 2.608 Å. The shortest intradimer Ir···Ir separation is 8.013 Å, and it is 3% greater than the shortest interdimer Ir···Ir separation of 7.786 Å. In addition, the iridium atoms are 0.1381 and 0.0967 Å out of the corresponding chloranilate coordination plane, and the distance is longer than that in complexes **5a** and **5b**. As shown in Figure 5c, the molecular rectangles stack via the *a*-axis to form rectangle channels due

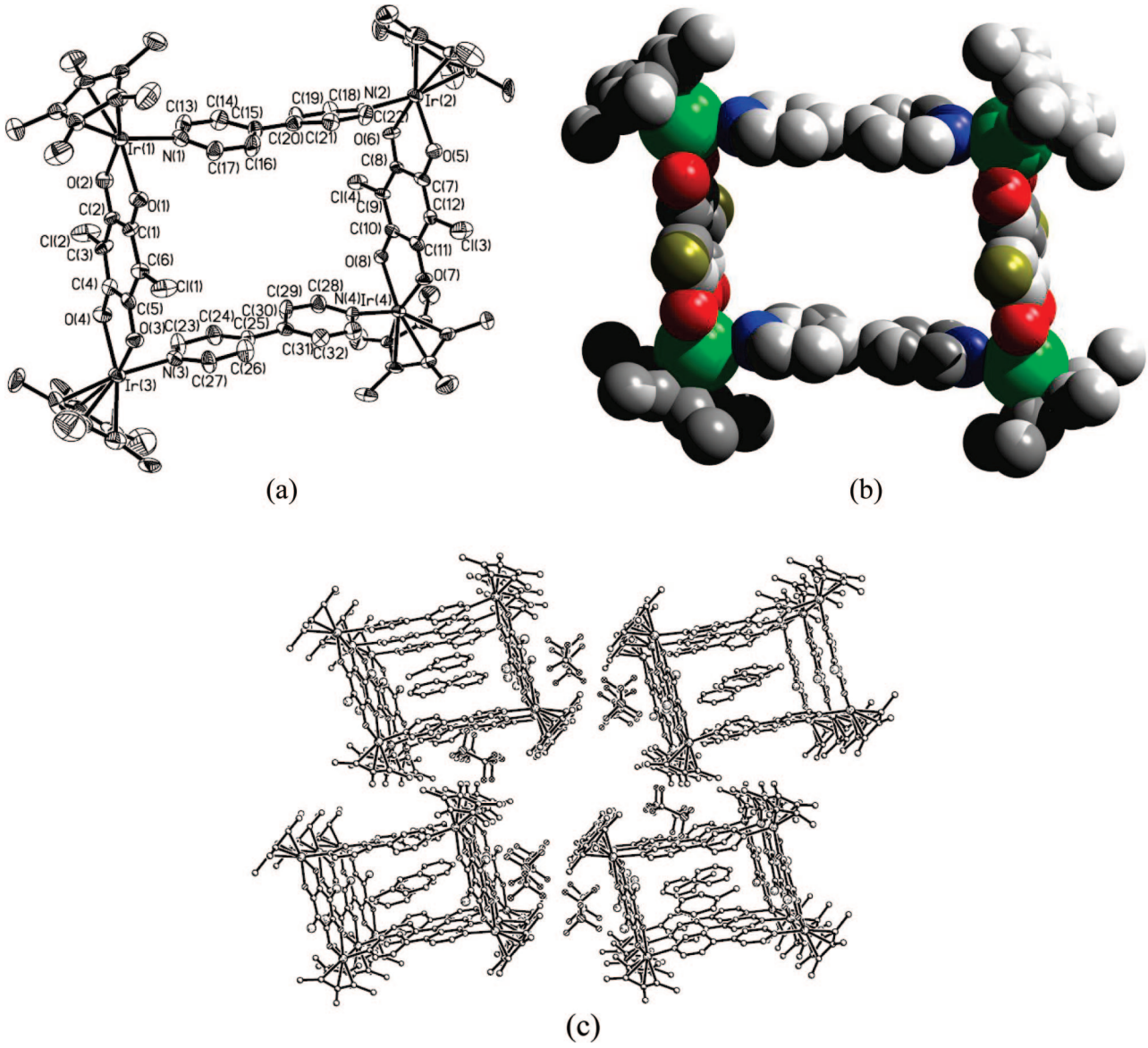

Figure 4. (a) Complex cation of **5b** with thermal ellipsoids drawn at the 30% level. (b) Space-filling model of cationic molecular rectangle **5b** based on its X-ray coordinates (Ir green; O red; N blue; C gray; Cl dark yellow). All hydrogen atoms, anions, and solvent molecules are omitted for clarity. (c) Stacking of the molecules in crystals of **5b** viewed along the *b*-axis; all hydrogen atoms are omitted for clarity.

to $\pi-\pi$ interactions between the independent molecules. The overall free voids are 30.7% of the cell volume, which is calculated on the condition that counteranions, solvent molecules, and hydrogen atoms are omitted. The counteranions are located outside of the channels.

Electrochemistry. The combination of the electrochemical activity and the complexation features of metallasupramolecular architectures could lead to attractive sensory materials. Unfortunately, however, only a few redox-active architectures of metallasupramolecules have been reported and reviewed by Koten et al. recently.[24]

The cyclic voltametric behavior of complexes **5b** and **5e** has been studied. The complex **5b** shows a good electrochemical response, and two obvious cathodic peaks and two anodic peaks can be observed in the voltammograms. As expected, the CV of **5b** shows a reversible one-electron oxidation at +0.25 V and a reversible one-electron reduction at −0.37 V versus Fc^+/Fc (ferrocinium/ferrocene) (anhydrous CH_2Cl_2, $(n\text{-}Bu)_4NPF_6$ as supporting electrolyte; see Figure 6a). The CV of **5e** shows three well-separated quasi-reversible one-electron transfer waves at $E_{1/2}$ = 0.27, −0.01, and −0.48 V vs SCE, which may be ascribed to ligand- and/or metal-centered processes (anhydrous CH_2Cl_2, $(n\text{-}Bu)_4NPF_6$ as supporting electrolyte; see Figure 6b).[15] These potentials suggest that the reduction products and oxidation products may be isolated through chemical reduction and oxidation reactions, respectively. We think that the chloranilate (CA) ligand is the most redox-active part in these complexes. The study of the redox chemistry of these systems is in progress in our group.

Conclusion

In conclusion, a new series of bi- and tetranuclear half-sandwich iridium complexes have been synthesized and characterized. The structures indicate that the tetranuclear iridium(III)

(24) Amijs, C. H. M.; van Klink, G. P. M.; van Koten, G. *Dalton Trans.* **2006**, 308.

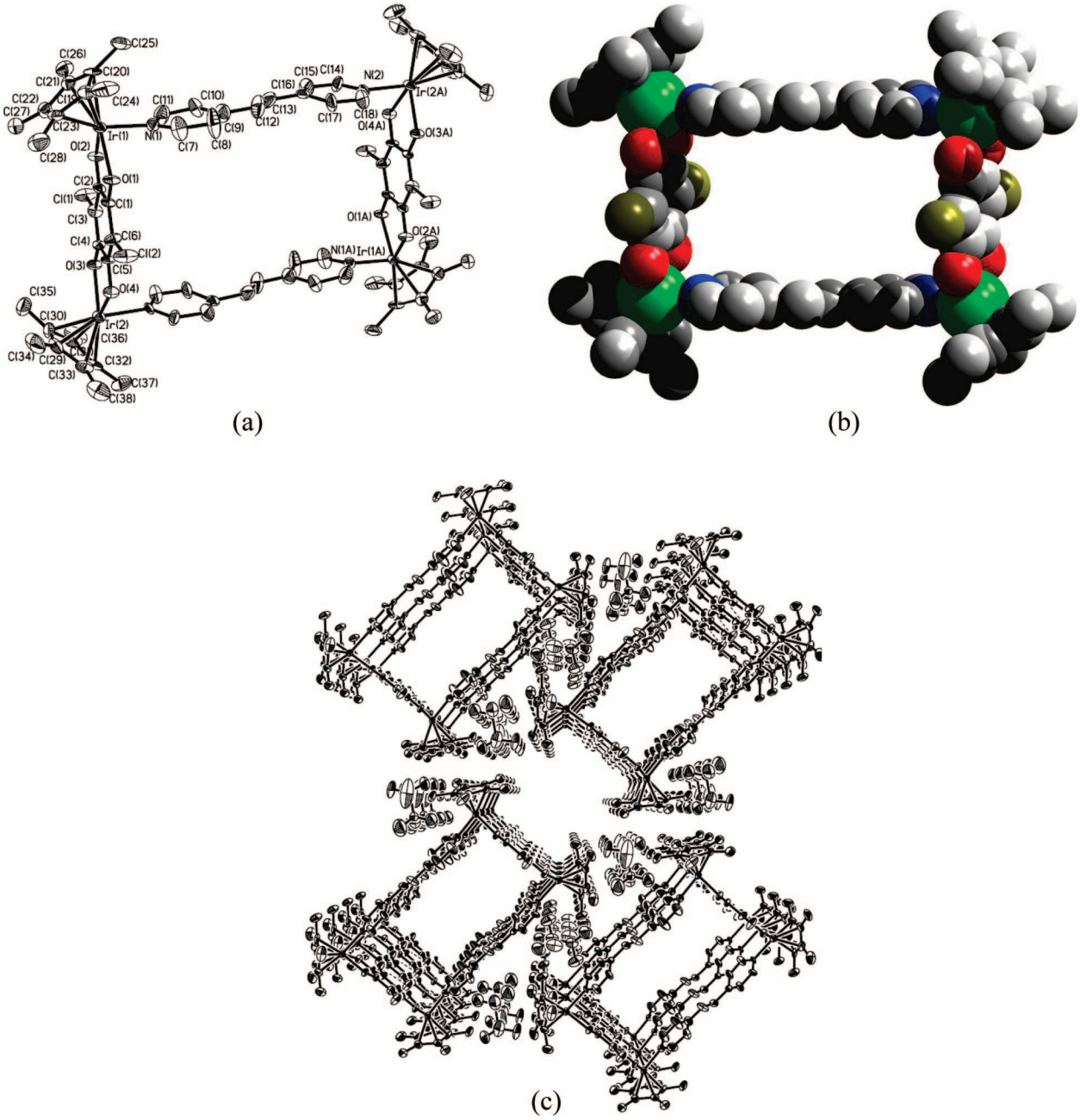

Figure 5. (a) Complex cation of **5e** with thermal ellipsoids drawn at the 30% level. (b) Space-filling model of cationic molecular rectangle **5e** based on its X-ray coordinates (Ir green; O red; N blue; C gray; Cl dark yellow). All hydrogen atoms, anions, and solvent molecules are omitted for clarity. (c) Stacking of the molecules in crystals of **5e** viewed along the *a*-axis. All hydrogen atoms are omitted for clarity.

complexes bear pentamethylcyclopentadienyl groups and two different ligands. The solvent molecules appeared between the independent rectangles or in the rectangle cavity according to the dimensions of the cavity. In addition, the electrochemical properties of **5b** and **5e** were investigated. We believe that when chloranilate as a bis-bidentate ligand is used, it will be possible to synthesize supramolecules with prism or cubic frameworks following this general strategy, and the work is in progress in our group.

Experimental Section

General Data. All manipulations were performed using standard Schlenk techniques under an atmosphere of nitrogen. CH_2Cl_2 was dried over CaH_2 and CH_3OH was distilled over Mg/I_2. THF, diethyl ether, hexane, and toluene were dried over Na and then distilled under nitrogen immediately prior to use. $[Cp^*IrCl_2]_2$[25] was prepared according to the literature. 2,5-Dichloro-3,6-dihydroxy-1,4-benzoquinone (chloranilic acid, H_2CA), 1,4-dibromobenzene, and pyridine 4-boronic acid were obtained from commercial sources and used without further purification.

The ^1H NMR spectra were measured on a VAVCE-DMX 400 spectrometer in CD_3OD. Elemental analysis was performed on an Elementar vario EL III analyzer, and the samples were dried under vacuum for 48 h before analyses. IR (KBr) spectra were recorded on the Nicolet FT-IR spectrophotometer. Electrochemical experiments were performed with a three-electrode system consisting of a platinum working electrode, a platinum wire counter electrode, and a silver wire as pseudoreference electrode. All potentials are reported versus the Fc^+/Fc couple. The measurements were carried

(25) White, C.; Yates, A.; Maitles, P. M. *Inorg. Synth.* **1992**, *29*, 228.

Table 5. Selected Bond Distances and Angles for 5e

Bond Distances (Å)			
Ir(1)−N(1)	2.072(9)	Ir(2)-N(2A)	2.111(8)
Ir(1)−O(1)	2.111(7)	Ir(1)−O(2)	2.121(7)
Ir(2)−O(3)	2.132(7)	Ir(2)−O(4)	2.152(7)
O(1)−C(1)	1.260(11)	O(2)−C(2)	1.255(12)
O(3)−C(4)	1.250(11)	O(4)−C(5)	1.267(12)
Cl(1)−C(3)	1.735(11)	Cl(2)−C(6)	1.725(12)
C(1)−C(2)	1.505(15)	C(1)−C(6)	1.417(15)
C(2)−C(3)	1.405(14)	C(3)−C(4)	1.375(15)
C(4)−C(5)	1.487(15)	C(5)−C(6)	1.361(15)
C(12)−C(13)	1.28(2)		
Bond Angles (deg)			
N(1)−Ir(1)−O(1)	84.3(4)	N(1)−Ir(1)−O(2)	85.7(3)
O(1)−Ir(1)−O(2)	75.6(3)	C(1)−O(1)−Ir(1)	116.3(7)
C(2)−O(2)−Ir(1)	116.4(7)	C(4)−O(3)−Ir(2)	115.4(7)
C(5)−O(4)−Ir(2)	115.4(7)	O(1)−C(1)−C(6)	124.3(10)
O(1)−C(1)−C(2)	115.8(9)	C(6)−C(1)−C(2)	119.9(9)
O(2)−C(2)−C(3)	125.8(11)	O(2)−C(2)−C(1)	115.5(9)
C(3)−C(2)−C(1)	118.7(10)	C(4)−C(3)−C(2)	120.8(10)
O(3)−C(4)−C(3)	122.3(10)	O(3)−C(4)−C(5)	118.0(9)
C(3)−C(4)−C(5)	119.7(9)	O(4)−C(5)−C(6)	122.5(11)
O(4)−C(5)−C(4)	115.6(9)	C(6)−C(5)−C(4)	121.9(10)
C(13)−C(12)−C(9)	128(2)	C(12)−C(13)−C(16)	129(2)

out under Ar, in degassed CH_2Cl_2 (distilled from CaH_2 under N_2), using 0.1 M $(n\text{-}Bu)_4NPF_6$ as the supporting electrolyte.

Preparation of Ligands. 4-(4-Bromophenyl)pyridine. To a 100 mL three-necked round-bottom flask equipped with a magnetic stirrer and a reflux condenser was added 1,4-dibromobenzene (10 mmol), and then pyridine 4-boronic acid (10 mmol), $Pd(dppf)_2Cl_2$ (0.5 mmol), and Na_2CO_3 (10 mmol) in toluene/water (1:1 v/v, 50 mL) were added. The mixture was degassed for 10 min and allowed to reflux for 72 h under N_2 atmosphere. The solvent was evaporated, and the residue was extracted with ethyl acetate followed by washing with water several times. The organic layer was dried over anhydrous $MgSO_4$ and evaporated to afford a pure brown solid, which was further purified by silica gel column chromatography [ethyl acetate/hexanes/triethylamine (5:5:1 v/v)] to afford pure 4-(4-bromophenyl)pyridine (yield, 67%). Anal. Calcd (%) for $C_{11}H_8BrN$: C 56.44, H 3.44, N 5.98. Found: C 56.42, H 3.38, N 6.01.

1,4-Bis(4-pyridyl)benzene. To a 100 mL three-necked round-bottom flask equipped with a magnetic stirrer and a reflux condenser was added 1,4-dibromobenzene (10 mmol), and then pyridine 4-boronic acid (35 mmol), $Pd(dppf)_2Cl_2$ (1 mmol), and Na_2CO_3 (20 mmol) in toluene/water (1:1 v/v, 50 mL) were added. The mixture was degassed for 10 min and allowed to reflux for 72 h under N_2 atmosphere. The solvent was evaporated, and the residue was extracted with ethyl acetate followed by washing with water several times. The organic layer was dried over anhydrous $MgSO_4$ and evaporated to afford a pure brown solid, which was further purified by silica gel column chromatography [ethyl acetate/hexanes/triethylamine (8:5:1 v/v)] to afford pure 1,4-bis(4-pyridyl)benzene (yield, 58%). Anal. Calcd (%) for $C_{16}H_{12}N_2$: C 82.73, H 5.21, N 12.06. Found: C 82.46, H 5.20, N 12.10.

Preparation of Dinuclear Complexes. $[Cp^*_2Ir_2(\mu\text{-}CA)Cl_2]$ (2). 2,5-Dichloro-3,6-dihydroxy-1,4-benzoquinone (H_2CA) (208 mg, 1 mmol) was added to a solution of CH_3ONa (108 mg, 2 mmol) in CH_3OH (80 mL). The mixture was stirred for 1 h, and $[Cp^*IrCl_2]_2$ (796 mg, 1 mmol) was added at room temperature. After stirring for 6 h, the solvent was removed, the residue was extracted with CH_2Cl_2, the filtrate was concentrated, and then diethyl ether was added, giving dark red crystals of **2** (755 mg, 81%). IR (KBr): ν_{CO} 1496 cm^{-1}. ^1H NMR (400 Hz, CD_3OD): δ 1.65 (s, 30H; Cp*). Anal. Calcd (%) for $C_{26}H_{30}Cl_4Ir_2O_4$: C 33.48, H 3.24. Found: C 33.42, H 3.18.

$[Cp^*_2Ir_2(\mu\text{-}CA)](CF_3SO_3)_2$ (3). $Ag(CF_3SO_3)$ (51 mg, 0.2 mmol) was added to a solution of **2** (93 mg, 0.1 mmol) in CH_3OH (20 mL) at room temperature and stirred for 15 h. The solvent was removed, the residue was extracted with CH_2Cl_2, the filtrate was concentrated, and diethyl ether was added, giving dark red crystals of **3** (108 mg, 93%). IR (KBr): ν_{CO} 1505 cm^{-1}. ^1H NMR (400 Hz, CD_3OD): δ 1.69 (s, 30H; Cp*). Anal. Calcd (%) for $C_{28}H_{30}Cl_2F_6Ir_2O_{10}S_2$: C 28.99, H 2.61. Found: C 28.64, H 2.59.

$[Cp^*_2Ir_2(\mu\text{-}CA)(pyridine)_2](CF_3SO_3)_2$ (4a). $Ag(CF_3SO_3)$ (51 mg, 0.2 mmol) was added to a solution of **2** (93 mg, 0.1 mmol) in CH_3OH (20 mL) at room temperature, and the mixture was stirred for 6 h, followed by filtration to remove undissolved compounds. Pyridine (16 mg, 0.2 mmol) was added to the filtrate, and the mixture was stirred for 10 h. The mixture was filtered, and the filtrate was concentrated to about 3 mL. Diethyl ether was added slowly into the red solution, giving red crystals of **4a** (117 mg, 89%). IR (KBr): ν_{CO} 1509 cm^{-1}; ^1H NMR (400 Hz, CD_3OD): δ 1.67 (s, 30H; Cp*), 7.64−8.65 (m, 12H; pyridine). Anal. Calcd (%) for $C_{38}H_{40}Cl_2F_6Ir_2N_2O_{10}S_2$: C 34.62, H 3.06, N 2.13. Found: C 34.52, H 3.09, N 2.02.

$[Cp^*_2Ir_2(\mu\text{-}CA)\{4\text{-}(4\text{-bromophenyl})\text{pyridine}\}_2](CF_3SO_3)_2$ (4b). $Ag(CF_3SO_3)$ (51 mg, 0.2 mmol) was added to a solution of **2** (93 mg, 0.1 mmol) in CH_3OH (20 mL) at room temperature, and the mixture was stirred for 6 h, followed by filtration to remove undissolved compounds. 4-(4-Bromophenyl)pyridine (47 mg, 0.2 mmol) was added to the filtrate, and the mixture was stirred for 10 h. The mixture was filtered, and the filtrate was concentrated to about 3 mL. Diethyl ether was added slowly into the red solution, giving red crystals of **4b** (136 mg, 84%). IR (KBr): ν_{CO} 1506 cm^{-1}. ^1H NMR (400 Hz, CD_3OD): δ 1.67 (s, 30H; Cp*), 7.63 (m, 4H; pyridyl), 7.89 (m, 4H; pyridyl), 8.26 (m, 4H; pyridyl), 8.58 (m, 4H; pyridyl). Anal. Calcd (%) for $C_{50}H_{46}Br_2Cl_2F_6Ir_2N_2O_{10}S_2$: C 36.88, H 2.85, N 1.72. Found: C 36.47, H 2.75, N 1.82.

Preparation of Tetranuclear Complexes. $[Cp^*_4Ir_4(\mu\text{-}CA)_2(\mu\text{-pyrazine})_2](CF_3SO_3)_4$ (5a). $Ag(CF_3SO_3)$ (51 mg, 0.2 mmol) was added to a solution of **2** (93 mg, 0.1 mmol) in CH_3OH (20 mL) at room temperature, and the mixture was stirred for 6 h, followed by filtration to remove undissolved compounds. Pyrazine (8 mg, 0.1 mmol) was added to the filtrate, and the mixture was stirred for 10 h. The mixture was filtered, and the filtrate was concentrated to about 3 mL. Diethyl ether was added slowly into the red solution, giving red crystals of **5a** (77 mg, 62%). IR (KBr): ν_{CO} 1508 cm^{-1}. ^1H NMR (400 Hz, CD_3OD): δ 1.67 (s, 60H; Cp*), 8.76 (s, 8H; pyrazine). Anal. Calcd (%) for $C_{64}H_{68}Cl_4F_{12}Ir_4N_4O_{20}S_4$: C 30.99, H 2.76, N 2.26. Found: C 30.85, H 2.71, N 2.27.

$[Cp^*_4Ir_4(\mu\text{-}CA)_2(\mu\text{-}4,4'\text{-dipyridyl})_2](CF_3SO_3)_4$ (5b): $Ag(CF_3SO_3)$ (51 mg, 0.2 mmol) was added to a solution of **2** (93 mg, 0.1 mmol) in CH_3OH (20 mL) at room temperature. The mixture was stirred for 6 h, followed by filtration to remove undissolved compounds. 4,4′-Dipyridyl (16 mg, 0.1 mmol) was added to the filtrate, and the mixture was stirred for 10 h. The solvent was removed, the residue was extracted with CH_2Cl_2, and the filtrate was concentrated to about 3 mL. Diethyl ether was added slowly into the red solution, giving red crystals of **5b** (85 mg, 65%). IR (KBr): ν_{CO} 1511 cm^{-1}. ^1H NMR (400 Hz, CD_3OD): δ 1.63 (s, 60H; Cp*), 8.04 (d, 8H; J = 6.0 Hz, dipyridyl), 8.53 (d, 8H; J = 6.0 Hz, dipyridyl). Anal. Calcd (%) for $C_{76}H_{76}Cl_4F_{12}Ir_4N_4O_{20}S_4$: C 34.68, H 2.91, N 2.13. Found: C 34.47, H 2.79, N 2.20.

$[Cp^*_4Ir_4(\mu\text{-}CA)_2\{\mu\text{-}2,5\text{-bis}(4\text{-pyridyl})\text{-}1,3,4\text{-oxadiazole}\}_2](CF_3SO_3)_4$ (5c). This complex (dark red, 78 mg, 49%) was obtained from **2** (93 mg, 0.1 mmol), $Ag(CF_3SO_3)$ (51 mg, 0.2 mmol), and 2,5-bis(4-pyridyl)-1,3,4-oxadiazole (22 mg, 0.1 mmol) by a procedure similar to that described for **5b**. IR (KBr): ν_{CO} 1512 cm^{-1}. ^1H NMR (400 Hz, CD_3OD): δ 1.68 (s, 60H; Cp*), 8.23 (d, 8H; J = 6.3 Hz, pyridyl), 8.65 (d, 8H; J = 6.3 Hz, pyridyl). Anal. Calcd (%) for $C_{80}H_{76}Cl_4F_{12}Ir_4N_8O_{22}S_4$: C 34.71, H 2.77, N 4.05. Found: C 34.26, H 2.75, N 4.25.

$[Cp^*_4Ir_4(\mu\text{-}CA)_2\{\mu\text{-}1,4\text{-bis}(4\text{-pyridyl})\text{benzene}\}_2(CF_3SO_3)_4$ (5d). This complex (dark red, 78 mg, 56%) was obtained from **2** (93 mg, 0.1 mmol), $Ag(CF_3SO_3)$ (51 mg, 0.2 mmol), and 1,4-bis(4-pyridyl)benzene (23 mg, 0.1 mmol) by a procedure similar to that

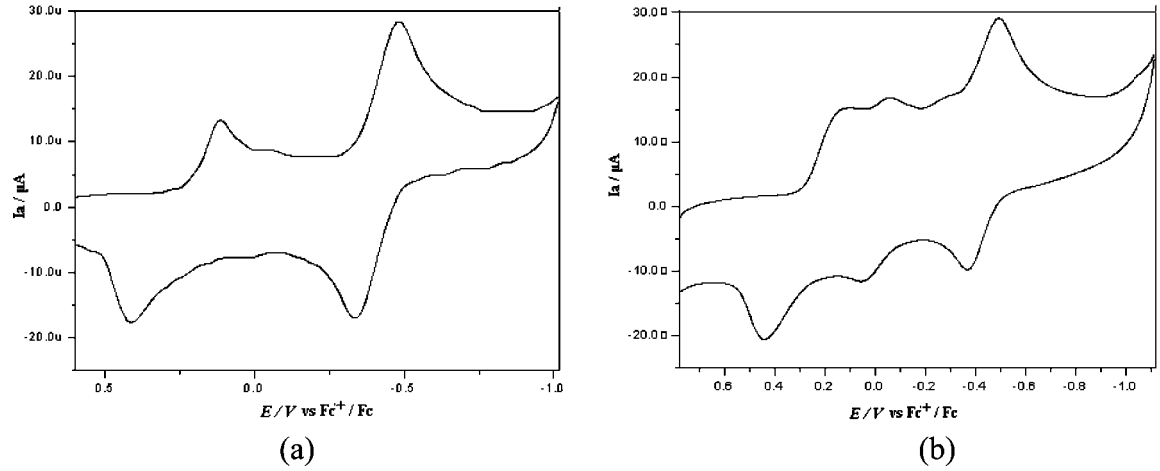

Figure 6. (a) Cyclic voltammogram of **5b** in anhydrous CH_2Cl_2 (0.1 M $(n\text{-}Bu)_4NPF_6$) at a scan rate of 100 mV s^{-1}. (b) Cyclic voltammogram of **5e** in anhydrous CH_2Cl_2 (0.1 M $(n\text{-}Bu)_4NPF_6$) at a scan rate of 100 mV s^{-1}.

Table 6. Crystallographic Data for Compounds 2, 4b, 5a, 5b, and 5e

	2 · $2CH_2Cl_2$	**4b** · CH_2Cl_2	**5a** · $C_6H_5CH_3$ · CH_2Cl_2 · $1.5CH_3OH$ · H_2O	**5b** · $C_6H_5CH_3$	**5e**
empirical formula	$C_{28}H_{34}Cl_8Ir_2O_4$	$C_{51}H_{48}Br_2Cl_4F_6Ir_2N_2O_{10}S_2$	$C_{73.5}H_{86}Cl_4F_{12}Ir_4N_4O_{22.5}S_4$	$C_{83}H_{84}Cl_4F_{12}Ir_4N_4O_{20}S_4$	$C_{80}H_{80}Cl_4F_{12}Ir_4N_4O_{20}S_4$
temperature (K)	173(2)	173(2)	173(2)	293(2)	293(2)
fw	1102.55	1713.05	2652.30	2724.38	2684.32
cryst size (mm^3)	0.12 × 0.10 × 0.08	0.15 × 0.12 × 0.10	0.10 × 0.10 × 0.08	0.15 × 0.10 × 0.08	0.15 × 0.12 × 0.10
cryst syst	monoclinic	monoclinic	orthorhombic	triclinic	triclinic
space group	*P*2(1)/*c*	*P*2(1)/*n*	*Pccn*	$P\bar{1}$	$P\bar{1}$
a (Å)	11.189(4)	12.952(6)	21.38(2)	15.502(5)	8.430(5)
b (Å)	20.083(6)	35.774(16)	29.82(3)	17.303(5)	16.397(10)
c (Å)	8.224(3)	14.664(6)	32.30(3)	22.752(7)	21.769(13)
α (deg)	90	90	90	71.007(4)	103.330(11)
β (deg)	107.958(4)	112.652(7)	90	77.715(5)	101.033(8)
γ (deg)	90	90	90	82.149(5)	99.267(8)
V ($Å^3$)	1757.9(10)	6270(5)	20587(32)	5623(3)	2807(3)
Z	2	4	8	2	1
ρ_{calcd} (g/cm^3)	2.083	1.815	1.712	1.609	1.588
μ(Mo Kα) (mm^{-1})	8.202	5.822	5.424	4.965	4.972
no. of collected reflns	8694	26 220	48 486	28 400	11 605
no. of unique reflns	3848	11 035	16 854	23 933	9659
no. of params	195	677	1134	1132	546
goodness of fit	1.044	1.062	0.888	0.838	0.937
R_1, wR_2 [$I > 2\sigma(I)$][a]	0.0277, 0.0619	0.0861, 0.1870	0.0651, 0.1303	0.0566, 0.1342	0.0590, 0.1342
R_1, wR_2 (all data)[a]	0.0355, 0.0643	0.1297, 0.2024	0.1324, 0.1497	0.1272, 0.1502	0.0991, 0.1457
max./min. residual density (e $Å^{-3}$)	2.614/−0.648	2.596/−1.924	3.349/−1.007	2.041/−1.496	2.346/−1.188

[a] $R_1 = \sum||F_o| - |F_c||$ (based on reflections with $F_o^2 > 2\sigma F^2$). $wR_2 = [\sum[w(F_o^2 - F_c^2)^2]/\sum[w(F_o^2)^2]]^{1/2}$; $w = 1/[\sigma^2(F_o^2) + (0.095P)^2]$; $P = [\max(F_o^2, 0) + 2F_c^2]/3$ (also with $F_o^2 > 2\sigma F^2$).

described for **5b**. IR (KBr): ν_{CO} 1508 cm^{-1}. ^1H NMR (400 Hz, CD_3OD): δ 1.69 (s, 60H; Cp*), 7.73 (m, 8H; pyridyl), 7.96 (m, 4H; pyridyl), 8.37 (m, 4H; pyridyl), 8.46 (m, 8H; pyridyl). Anal. Calcd (%) for $C_{88}H_{84}Cl_4F_{12}Ir_4N_4O_{20}S_4$: C 37.96, H 3.04, N 2.01. Found: C 35.43, H 2.83, N 2.42.

[Cp*$_4$Ir$_4$(*μ*-CA)$_2${*μ*-(*E*)-1,2-bis(4-pyridyl)ethene}$_2$(CF$_3$SO$_3$)$_4$ (5e). This complex (dark red, 90 mg, 67%) was obtained from **2** (93 mg, 0.1 mmol), $Ag(CF_3SO_3)$ (51 mg, 0.2 mmol), and (*E*)-1,2-bis(4-pyridyl)ethene (18 mg, 0.1 mmol) by a procedure similar to that described for **5b**. IR (KBr): ν_{CO} 1504 cm^{-1}. ^1H NMR (400 Hz, CD_3OD): δ 1.66 (s, 60H; Cp*), 7.52 (m, 8H; dipyridyl), 7.78 (s, 4H; aryl), 8.35 (m, 8H; dipyridyl). Anal. Calcd (%) for $C_{80}H_{80}Cl_4F_{12}Ir_4N_4O_{20}S_4$: C 35.79, H 3.00, N 2.09. Found: C 35.43, H 2.83, N 2.32.

X-ray Crystallography. Suitable crystals for X-ray analysis of **2**, **4b**, and **5e** were obtained by slow diffusion of diethyl ether/hexane into CH_2Cl_2 solutions of the corresponding compound. A suitable crystal for X-ray analysis of **5a** was recrystallized from toluene/CH_2Cl_2/CH_3OH, and **5b** was obtained by slow diffusion of toluene into CH_2Cl_2 solutions. The measurements were made by using Mo Kα radiation at −100 °C under a cold nitrogen stream except for **5b** and **5e**. Details of the data collection and refinement are summarized in Table 6. All structures were solved by Patterson methods. The positions of all non-hydrogen atoms except the solvent molecules were refined with anisotropic thermal parameters by using full-matrix least-squares methods. The structures were solved by direct methods using SHELX-97 and refined by full-matrix least-squares calculations, using the SHELXTL-97 program system.[26]

In complex **2**, all non-hydrogen atoms were refined anisotropically. In complex **4b**, some disordered solvents had to be omitted by using the SQUEEZE algorithm.[27] Except atom C29 and one of the two triflate anions (because of nonpositive definition), other non-hydrogen atoms were refined anisotropically. In complex **5a**, the SQUEEZE algorithm was also used to omit the disordered solvents. Non-hydrogen atoms were refined anisotropically except atom C46 because of the nonpositive definition. All the hydrogen

(26) Sheldrick, G. M. *SHELXL-97*; Universität Göttingen: Germany, 1997.

(27) van der Sluis, P.; Spek, A. L *Acta Crystallogr.* **1990**, *A46*, 194.

atoms of the hydroxy group in methanol solvent molecules and hydrogen atoms of the methyl fragment of one methanol molecule were not found. In complex **5b**, some solvent molecules were disordered and could not be refined properly. Hence, the SQUEEZE algorithm had to be used to omit them. Two of four pentamethylcyclopentadienyl ligands in the cation were disordered because of rotation at room temperature. They were refined to two idealized positions (52:48). Two of the four anions and a toluene solvent molecule in the asymmetric unit were refined isotropically because of the nonpositive definition, and other non-hydrogen atoms were refined anisotropically. In complex **5e**, one-fourth of the triflate anions and other solvent molecules were strongly disordered. Therefore, new data sets corresponding to omission of the missing anions and solvents were generated with the SQUEEZE algorithm and the structures were refined to convergence. All of the non-hydrogen atoms were refined anisotropically. In all complexes, hydrogen atoms that could be found were placed in the geometrically calculated positions with fixed isotropic thermal parameters.

Crystal data, data collection parameters, and the results of the analyses of compounds **2**, **4b**, **5a**, **5b**, and **5e** are listed in Table 6.

Acknowledgment. Financial support by the National Science Foundation of China (20531020, 20421303, 20771028), by Shanghai Leading Academic Discipline Project (B108), and by Shanghai Science and Technology Committee (06XD14002) is gratefully acknowledged.

Supporting Information Available: The crystallographic data for **2**, **4b**, **5a**, **5b**, and **5e** are available free of charge via the Internet at http//www.pubs.acs.org.

OM800426E